Yuzuncu Yil University Journal of the Institute of Natural & Applied Sciences

https://dergipark.org.tr/en/pub/yyufbed

Research Article

Assessment of Adsorption Process and Mechanism for Methylene Blue Removal on Cranberry: Isotherm, Kinetic and Thermodynamic Studies

Ali Rıza KUL[1], Adnan ALDEMİR[2*]

[1]Van Yüzüncü Yıl University, Faculty of Science, Chemistry Department, 65080, Van, Türkiye

[2]Van Yüzüncü Yıl University, Faculty of Engineering, Industrial Engineering Department, 65080, Van, Türkiye

*Corresponding author e-mail: adnanaldemir@yyu.edu.tr

Abstract: In the present study, cranberry based adsorbent (CBA) was used for the removal of Methylene Blue (MB) from aqueous solutions. The influences of operational parameters, including initial MB concentration (15–75 mg L^{-1}), temperature (298 K–318 K) and contact time (10–180 min), were systematically examined. The removal efficiencies at the 35 mg L^{-1} initial MB concentration were determined to be 79.3%, 82.9% and 85.8% at the 298 K, 308 K and 318 K, respectively. The maximum adsorption capacity (q_m) was achieved at 91.743 mg g^{-1} at 318 K. Experimental data were evaluated using adsorption isotherm models, kinetic studies and thermodynamic analyses. Temkin model was provided the best fit to the experimental data among the applied four isotherm models (Langmuir, Freundlich, Dubinin–Radushkevich and Temkin). Adsorption kinetics were evaluated with three models and adsorption process was followed the pseudo second order (PSO) kinetic model most accurately, which has the highest R^2 values. Thermodynamic analysis for adsorption of 65 mg L^{-1} initial MB concentration at 318 K was revealed negative values for Gibbs free energy (-2942.16 J mol^{-1}), along with positive enthalpy values (16618.02 J mol^{-1}) and entropy (61.51 J $mol^{-1}K^{-1}$). These results were showed that adsorption process was spontaneous and endothermic in nature and the activation energy was calculated to be 14.44 kJ mol^{-1}. These results suggested that prepared cranberry adsorbents was represented a promising low-cost alternative to conventional adsorbents for effective removal of dye pollutants from wastewater.

Keywords: Adsorption, Isotherm, Kinetic, Thermodynamic, Methylene Blue

Kızılcık ile Metilen Mavisi Giderimi için Adsorpsiyon Proses ve Mekanizmasının Değerlendirilmesi: İzoterm, Kinetik ve Termodinamik Çalışmaları

Özet: Bu çalışmada Metilen Mavisinin (MB) sulu çözeltilerden giderimi için kızılcık ile hazırlanan adsorbent (CBA) kullanıldı. Başlangıç MB derişimi (15–75 mg L^{-1}), sıcaklık (298 K–318 K), ve temas süresi (10–180 dk) çalışma parametrelerinin etkileri araştırıldı. 35 mg L^{-1} başlangıç MB derişimi için giderim değerleri 298 K, 308 K ve 318 K' de sırasıyla %79,3, %82,9 ve %85,8 olarak belirlendi. 318 K'de en yüksek adsorpsiyon kapasitesi (q_m) 91,743 mg g^{-1} olarak elde edildi. Deneysel veriler izoterm model, kinetik çalışmalar ve termodinamik analizler ile değerlendirildi. Temkin modeli, dört izoterm model (Langmuir, Freundlich, Dubinin–Radushkevich ve Temkin) arasından deneysel verilere en uygun model olarak belirlendi. Adsorpsiyon kinetiği üç model ile değerlendirildi ve adsorpsiyon prosesi en yüksek korelasyon katsayısı (R^2) değerlerine sahip yalancı ikinci derece (PSO) kinetik model ile açıklandı. 318 K'de 65 mg L^{-1} başlangıç MB derişimi için yapılan termodinamik hesaplamalarda negatif Gibbs serbest enerji değeri (-2942.16 J mol^{-1}), pozitif enthalpi değeri (16618,02 J mol^{-1}) ve pozitif entropi değeri (61,51 J $mol^{-1}K^{-1}$) elde edildi. Bu sonuçlara göre adsorpsiyon prosesinin spontane ve endotermik yapıda olduğu belirlendi ve adsorpsiyon olayının aktivasyon enerjisi 14,44 kJ mol^{-1} olarak hesaplandı. Bu bulgular atıksulardan boya kirliliklerinin etkili giderimi için klasik adsorbentlere alternatif olarak düşük maliyetli kızılcık ile hazırlanan adsorbentin kullanılabileceğini göstermiştir.

Anahtar Kelimeler: Adsorpsiyon, İzoterm, Kinetik, Termodinamik, Metilen Mavisi

Received Date:28.10.2025
Accepted Date: 19.01.2026

How to cited: Kul, A, R. and Aldemir A. (2026). Assessment of Adsorption Process and Mechanism for Methylene Blue Removal on Cranberry: Isotherm, Kinetic and Thermodynamic Studies. *Yuzuncu Yil University Journal of the Institute of Natural and Applied Sciences, 31* 1-18. https://doi.org/10.53433/yyufbed.1812282

1. Introduction

Water is an essential resource for continuity of life; however, the escalation of industrial and agricultural activities over recent decades has significantly contributed to the contamination of natural water sources worldwide. In contemporary times, the preservation of water resources has emerged as a critical global issue, closely linked to ensuring the safety of the planet and the future of humanity (Daneshvar et al., 2017; Das et al., 2023). Rapid industrialization and population growth have been primary drivers of water pollution, particularly in developing regions. One of the current major challenges in wastewater treatment is the effective removal of persistent organic pollutants, which are extensively employed across various industrial domains such as the food, textile, cosmetic and paper industries (Mladenov et al., 2022). Industrial dye pollution, in particular, poses a severe threat to environmental integrity and the health of living organisms (Aigbe et al., 2021).

Dyes which are organic compounds are utilized in a wide range of manufacturing sectors, including textiles, plastics, pharmaceuticals, paper production, printing, rubber, leather, paints, cosmetics, food and pulp industries (Singh et al., 2015; Alver et al., 2020; Kul et al., 2023). These compounds are highly soluble in water and typically utilized in granular or powdered forms. Many synthetic dyes are chemically stable and resistant to degradation, with the potential to generate mutagenic and carcinogenic by products (Spagnoli et al., 2017). Recent studies have highlighted growing concerns over the direct discharge of dyes into natural ecosystems, which are given their toxicological effects on humans, animals and the environment (Dhaouadi et al., 2020; Liu et al., 2020). Even at trace levels, they can severely impact aquatic ecosystems and human health by altering the physicochemical properties of water bodies. Their persistence and carcinogenic nature render them difficult to degrade and excessive human exposure may result in poisoning, skin irritation, allergic reactions and cancer. Therefore, the removal of dyes from industrial wastewater is of paramount environmental importance (Chowdhury et al., 2023).

Various treatment technologies such as oxidation processes (Kang et al., 2019; Muniyasamy et al., 2020), membrane separation, ozonation (Zhang et al., 2024), electrochemical methods (Pereira et al., 2020; Alsaffar et al., 2023), ion exchange (Joseph et al., 2020), coagulation-flocculation (Ayhan et al., 2024; Aldemir et al., 2021) and adsorption (Salleh et al., 2011; Yagub et al., 2014; Aldemir et al., 2023; Kul et al., 2023) have been employed for dye removal from wastewater (Ahmad et al., 2015; Katheresan et al., 2018). Nonetheless, many of these methods have disadvantages such as high operational costs, generation of secondary pollutants and limited removal efficiencies, despite their partial success.

Adsorption has gained prominence due to its simplicity, cost-effectiveness and high removal efficiency, making it a preferred method for wastewater treatment (Bhatti et al., 2020; Demirci et al., 2024). The adsorbent has an important role in the success of adsorption processes. Materials such as zeolites, activated carbon and graphene-based composites have been widely studied because of their high surface area, porosity and ion exchange capabilities (Dutta et al., 2021). But the high cost of the production and regeneration processes of these adsorbents have led to growing interest in exploration of affordable, environmentally friendly and renewable alternatives. In this context, numerous agricultural by products such as rice husk, sugarcane bagasse, eucalyptus bark sawdust, pine needles and fruit kernel powder have been investigated as low-cost adsorbents for the removal of various organic and inorganic contaminants from aqueous environments (Zeghioud et al., 2022).

Methylene Blue (MB) is widely used in industrial applications, particularly in the coloring of cotton, wool and silk fabrics. Known chemically as 3,7-bis(dimethylamino) phenothiazine chloride or tetramethylthionine chloride, MB is also employed in food, cosmetic and pharmaceutical applications (Jawad et al., 2019). Nevertheless, the release of MB polluted effluents into environment raises significant health concerns. Exposure to MB has been linked to a range of health effects, including cyanosis, tissue necrosis, Heinz body formation, jaundice, vomiting, shock and elevated heart rate in humans (Khan et al., 2022; Peighambardoust et al., 2022). Moreover, MB adversely affects plant life, as observed in species like Spirulina platensis and Chlorella vulgaris, where it causes inhibited growth, pigment degradation and elevated protein content (Oladoye et al., 2022). In addition to impairing the aesthetic quality of water by altering its color, dyes hinder photosynthetic activity in aquatic plants and algae, thereby disrupting ecological balance (Misran et al., 2024). Given these concerns, the efficient

removal of MB from water is critical to ensuring sustainability and safeguarding health. The aim of this study is evaluated the MB adsorption efficiency of cranberry adsorbent (CBA) as a low-cost and environmental friendly material in aqueous media. MB is selected as the model contaminant due to its widespread use and known its adverse effects on health and environment. Within the scope of this research, adsorption isotherms, kinetic models and thermodynamic parameters associated with the interaction between MB and CBA are systematically evaluated. The novelty of this study is investigated the adsorption performance of CBA which is biomass based material for the removal of MB from wastewater.

2. Materials and Method

2.1. Preparation of adsorbent (CBA) and MB solutions for adsorption

The cranberry adsorbent (CBA) was prepared and utilized in batch adsorption experiments. Cranberries were collected from trees grown at the Olur/Erzurum, Türkiye. After collection the cranberries were washed and dried at the 25°C for 48 hours. Dried cranberries were crushed and ground into a powder, which was sieved to obtain particles with a size 230 mesh. Prepared CBA was stored in plastic containers for experiments.

MB was used as adsorbate which chemical formula is $C_6H_{18}N_3SCl.3H_2O$ and molecular weight is MW 319.85 g/mol. 1 g L^{-1} MB stock solution was prepared by distilled water and 15, 25, 35, 45, 55, 65 and 75 mg L^{-1} MB solutions were prepared by the dilution of stock solution. MB and other chemicals used for the experiments was purchased from Merck Chemicals Company and used without purification.

2.2. Adsorption experiments

The 1000 mL of MB solutions were treated with the CBA in a water bath. All experiments were conducted with 3.0 g of CBA per liter and pH 6.5 conditions which were determined through preliminary experiments. The MB concentrations in aqueous solutions were measured over a period of 180 minutes. After removal process, suspensions were centrifuged at 5000 rpm and supernatants were analyzed using a UV-VIS spectrophotometer (PG Instruments Ltd. T80) at a wavelength of 660 nm. The experiments were carried out in duplicate and averages of experimental data were used for calculations. MB concentrations in the solutions were obtained with a calibration curve, which was generated from MB solutions varied from 0 to 100 mg L^{-1} concentrations. The equilibrium amount of MB (q_e) adsorbed on the CBA was calculated using Eq. (1):

$$q_e = \frac{(C_0 - C_e)\,V}{m} \tag{1}$$

where V, C_0, C_e and m represents the solution volume (L), initial and equilibrium MB concentrations (mg L^{-1}) and CBA mass (g), respectively. Removal percentages of MB were calculated with Eq. (2):

$$Removal\ percentage\ (\%) = \frac{(C_0 - C_e)}{C_0} * 100 \tag{2}$$

The adsorption of MB on CBA was investigated with respect to the initial MB concentrations, temperature and contact time. Isotherm, kinetic and thermodynamic calculations for adsorption of MB on CBA were analyzed using the data obtained from the study.

2.3. Isotherm studies of adsorption

Isotherm models are providing valuable outputs for the interaction mechanisms between adsorbent surfaces and adsorbate species (Parlayici & Aras, 2024). Each model offers a different theoretical framework to describe the nature of the adsorption. In this research, four isotherm models Freundlich, Langmuir, Temkin and Dubinin-Radushkevich (D–R) are applied to evaluate the adsorption characteristics of Methylene Blue (MB) onto cranberry adsorbent (CBA). Langmuir model is usable that

adsorption occurs uniformly over a monolayer process without interactions between adsorbed molecules. Mathematical expression of this isotherm is showed in Eq. (3);

$$q_e = (q_m K_L C_e)/(1 + K_L C_e) \quad (3)$$

Here, q_{max} is the maximum adsorption capacity (mg g^{-1}) and K_L is Langmuir constant (L g^{-1}). These parameters are derived from a linear plot of C_e/q_e against C_e (Kul et al., 2023). Additionally, the separation factor (R_L) which is calculated with Eq. (4), indicates the favorability of adsorption process;

$$R_L = \frac{1}{1 + K_L Ce} \quad (4)$$

The R_L values between 0 and 1 suggest that adsorption is favorable. Freundlich isotherm is explained with the adsorption occur on systems involving heterogeneous surfaces. It is expressed in Eq. (5);

$$q_e = K_F Ce^{1/n} \quad (5)$$

where K_F is denoted the Freundlich constant related to adsorption capacity and n is a value of adsorption intensity, both derived from logarithmic plot of q_e versus C_e (Aldemir et al., 2023). Temkin isotherm is demonstrated adsorbate–adsorbent interactions and proposes that heat of adsorption decrease linearly as coverage increase of temperature which is given by Eq. (6);

$$q_e = Bln(K_T C_e) \quad (6)$$

where K_T is correspond to the equilibrium binding constant and B is associated with adsorption heat, defined by Eq. (7);

$$B = RT/b_T \quad (7)$$

where R is universal gas constant, T is absolute temperature (K) and b_T is relate to the adsorption potential. Dubinin–Radushkevich (D–R) isotherm is explain the assessment of adsorption mechanism involving heterogeneous surfaces and to evaluate the mean free energy of adsorption. This model is formulated in Eq. (8);

$$ln(q_e) = ln(q_m) - K_D * \varepsilon^2 \quad (8)$$

where q_m is the theoretical saturation capacity (mg g^{-1}), K_D is the D–R constant (mol² kJ^{-2}) and ε is the Polanyi potential, calculated with Eq. (9);

$$\varepsilon = RTln[1 + (1/Ce)] \quad (9)$$

The mean adsorption energy E (kJ mol^{-1}) is determined with Eq. (10);

$$E = 1/\sqrt{2K_D} \quad (10)$$

E is help to distinguish between physical and chemical adsorption processes with values of E below 8 kJ mol^{-1} show that physical adsorption, between 8 and 16 kJ mol^{-1} indicate that a physicochemical process and those exceeding 16 kJ mol^{-1} suggest that chemical adsorption (Kul & Aldemir, 2025). The adsorption parameters obtained with four isotherm models are given in Table 2 and comparison of MB adsorption performance of CBA with some different adsorbents is given in Table 3. Four isotherm plots of MB adsorption on CBA are illustrated in Figure 4.

2.4. Kinetic studies of adsorption

The kinetics of MB adsorption on CBA are examined with pseudo first order (PFO), pseudo second order (PSO) and intraparticle diffusion (IPD) kinetic models. These models are applied to the

15, 25, 35, 45, 55, 65, 75, mg L^{-1} initial MB concentrations. The quantity of adsorbed dye amount at specific time intervals (q_t) is determined with Eq. (11);

$$q_t = \frac{(C_0 - C_t)\,V}{m} \tag{11}$$

where, C_t represent the MB concentration, V is MB solution volume (L) and m is adsorbent mass (g). The PFO model which is initially proposed by Lagergren, assume that rate of occupancy of adsorption sites is the number of unoccupied sites. PFO model is represented by Eq. (12);

$$ln(q_e - q_t) = lnq_e - k_1 t \tag{12}$$

where k_1 is the rate constant (min^{-1}) and it can be obtained by plotting $\ln(q_e - q_t)$ versus time t (Lagergren, 1898). The PSO model is used to describe the relationship between adsorbent and solute molecules of adsorption mechanism and it is given by Eq. (13);

$$\frac{t}{q_t} = \frac{1}{(k_2 q_e^2)} + \frac{t}{q_e} \tag{13}$$

where k_2 (g mg^{-1} min^{-1}) is the rate constant, determined from the linear plot of t/q_t against t (Ho and McKay, 1999). IPD kinetic model is the rate-limiting step, which is given with Eq. (14);

$$q_t = k_{ipd} t^{0.5} + C \tag{14}$$

where k_{ipd} (mg g^{-1} $min^{0.5}$) is indicated that diffusion rate constant and C is correspond to the boundary layer thickness. These parameters are obtained from the linear relationship between q_t and $t^{0.5}$ (Weber & Morris, 1963). The kinetic parameters obtained from these models for 65 mg L^{-1} MB concentration are given in Table 4. The plots of PFO, PSO and IPD models, based on experimental data at 318 K, are shown in Figure 5.

2.5. Thermodynamic studies of adsorption

Gibbs free energy (ΔG°), enthalpy (ΔH°) and entropy (ΔS°) values are play a crucial role in understanding influence of temperature on adsorption behaviour. These parameters are obtained with the thermodynamic equations given in Eqs. (15)–(17);

$$\Delta G^{\circ} = -RTlnK_d \tag{15}$$

$$\Delta G^{\circ} = \Delta H^{\circ} - T\Delta S^{\circ} \tag{16}$$

$$lnK_d = \frac{\Delta S^{\circ}}{R} - \frac{\Delta H^{\circ}}{RT} \tag{17}$$

In these expressions, K_d (L g^{-1}) is represented the distribution coefficient, which is calculated by plotting the ratio of q_e/C_e against q_e. ΔH° and ΔS° values are extracted from slope and intercept of a plot of $\ln K_d$ versus 1/T. The activation energy (E_A) is provided further insight into nature of adsorption mechanism. E_A in range of 0–40 kJ mol^{-1} typically evidences a physical adsorption, whereas values between 40 and 800 kJ mol^{-1} are characteristics of chemical adsorption. Activation energy of MB adsorption on CBA is determined with Arrhenius equation which is given in Eq. (18);

$$lnk_2 = lnA - \frac{E_A}{RT} \tag{18}$$

where, k_2 is rate constant (g mol^{-1} s^{-1}), A is Arrhenius factor (g mol^{-1} s^{-1}), E_A is activation energy (J mol^{-1}), R is universal gas constant (J mol^{-1} K^{-1}) and T is absolute temperature (K).

3. Results and Discussion

3.1. Effect of contact time and initial dye (MB) concentration

The contact time between adsorbent particles and adsorbate molecules plays an important role in the adsorption experiments. The influences of both initial MB concentrations (15–75 mg L^{-1}) and contact time on adsorption were analyzed at the 298 K, 308 K and 318 K. The results were illustrated in Figure 1, which were showed the impact of MB adsorption on CBA with time and initial MB concentrations. The MB removal efficiencies were increased with contact time up to 120 minutes. During the initial stages, the adsorption was rapid because the adsorbent pores were initially empty and they were filled up gradually over time. The rate of dye removal was slowed down until equilibrium and it was stabilized after reaching saturation. For 45 mg L^{-1} initial MB concentration, the equilibrium adsorption (q_e) was increased from 10.78 mg g^{-1} at 5 minutes to 19.32 mg g^{-1} at 120 minutes, indicated that adsorbent progressively adsorbed more dye molecules until saturation. Also, removal percentages of MB were increased with higher initial MB concentrations, suggested that more active sites on adsorbent surface were available for adsorption. CBA removal capacity of MB concentration increase from 15 to 75 mg L^{-1} was increased as 5.88 to 27.73 mg g^{-1} for 298 K, 5.95 to 28.91 mg g^{-1} for 308 K and 6.01 to 30.45 mg g^{-1} for 318 K. The best removal percentages of MB adsorption were obtained to 79.3 %, 82.9 % and 85.8 % for 35 mg L^{-1} at the 298 K, 308 K and 318 K, respectively. Changes in initial MB concentration with contact time were observed differences in removal percentages of CBA.

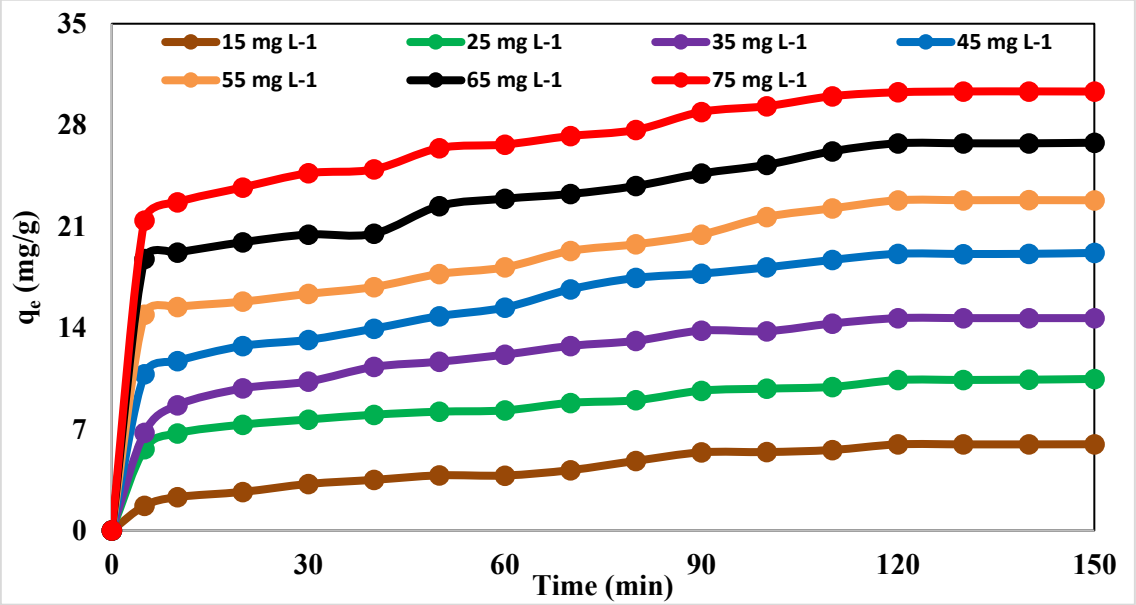

Figure 1. Effect of the contact time for adsorption of MB on CBA (temp: 318 K).

3.2 Effect of temperature

The effect of temperature for MB adsorption on CBA is shown in Figure 2. The removal percentages for seven MB concentrations at three temperatures are given in Table 1. The results were demonstrated that adsorption rate of MB improved with increasing temperature. This enhancement was attributed to increased mobility of MB molecules at higher temperatures, which were boosted their kinetic energy and accelerated their motion within the solution. As a result, dye molecules were more readily reached the adsorbent's mesoporous structures, which were offered greater surface area for adsorption. Additionally, elevated temperatures were reduced the viscosity of solution, which were further facilitated the diffusion of dye molecules through solution. This enhanced mobility was enabled the molecules to interact more effectively with the adsorbent surface. Among the different concentrations, 15 mg L^{-1} initial dye solution was yielded the highest removal percentages for three process temperatures. Removal efficiencies of MB were decreased with increasing initial MB

concentrations. Furthermore, removal efficiencies were increased as temperature increased for seven applied MB concentrations. The maximum removal percentages were achieved at 318 K which was studied the highest temperature. These results were compared with the previous studies, which also observed that an increase in temperature lead to greater MB adsorption for various adsorbents (Demirci et al., 2024). This temperature dependent adsorption behaviour was supported the conclusion that removal process was endothermic in nature. The temperature changes in both equilibrium concentrations and adsorbed amounts of MB are shown in Figure 3 and they are highlighting the direct relationship between temperature and removal percentages.

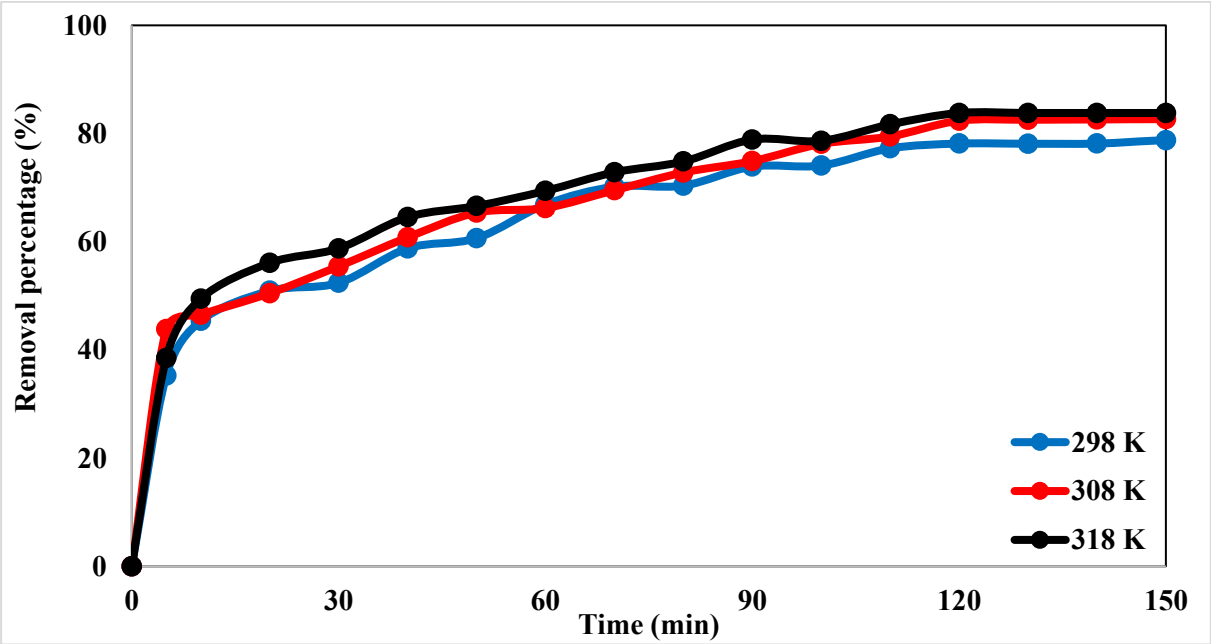

Figure 2. Effect of temperature for MB removal on CBA (C_0: 35 mg L^{-1}).

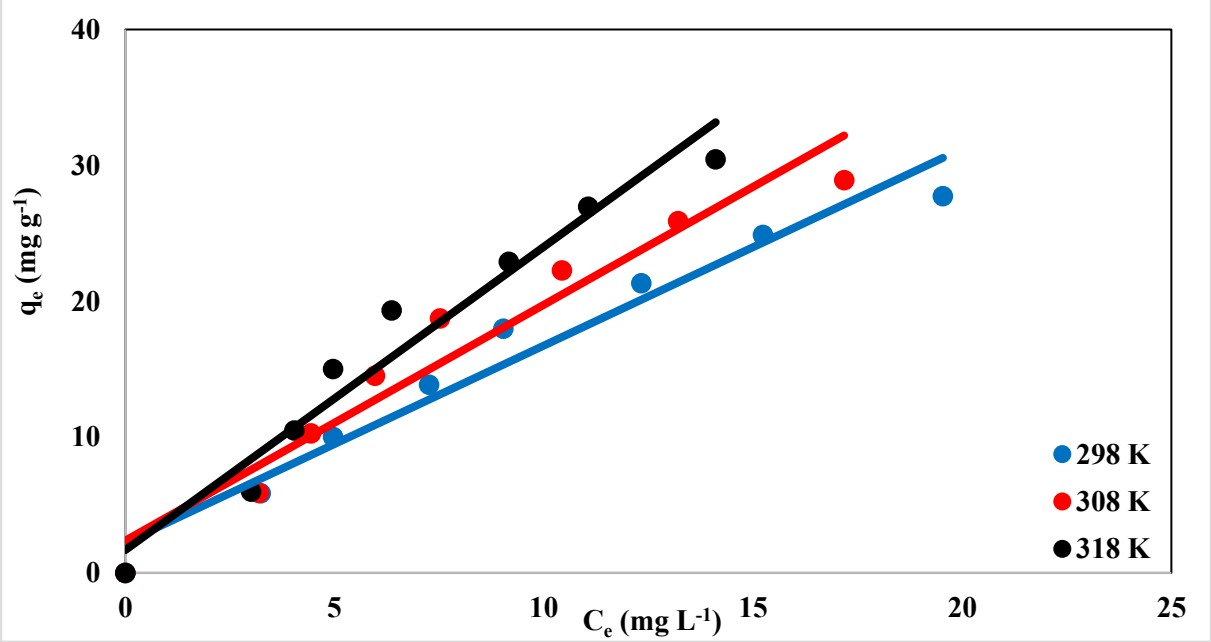

Figure 3. Effect of temperature for changes of equilibrium and adsorbed amounts of MB.

Table 1. Removal percentages of MB adsorption on CBA.

Initial dye concentration (mg L^{-1})	Removal percentage (%)			
	298 K	308 K	318 K	R^2
15	79.911	83.289	85.844	0.996
25	79.120	82.240	84.760	0.997
35	79.257	81.943	84.150	0.985
45	78.400	81.543	83.732	0.991
55	77.582	81.018	83.327	0.993
65	76.554	79.677	82.985	0.989
75	73.947	77.093	81.187	0.994

3.3 Isotherm results of MB adsorption on CBA

Equilibrium isotherms are evaluated for the chemical affinity between adsorbate and adsorbent, help to investigate the interactions to the structural features of the molecules. Determining the most appropriate isotherm model is important to modeling and optimization of adsorption process (Wang & Guo, 2020). In this study, adsorption of MB on CBA in aqueous phase was investigated to evaluate the adsorption capacity and behavior of CBA. Four isotherm models (Freundlich, Langmuir, Temkin and Dubinin-Radushkevich (D-R) were used to characterize the interactions between MB and CBA. These models are help the explain different adsorption mechanisms, such as surface homogeneity, multilayer formation, or the energy of adsorption sites. The obtained data were tested to each of these models with their equations. Four isotherm plots were shown in Figure 4 and the calculated parameters of four isotherms were listed in Table 2. Temkin isotherm was provided the best fit to obtained data, as indicated that its the highest R^2 values compared to other models. This result was suggested that MB adsorption onto CBA occurs on a heterogeneous surface and this process was involved multilayer adsorption, consistent with assumptions of the Temkin model. The values of Temkin constant (b_T) and binding constant (K_T) of isotherm are listed in Table 2. K_T values, which can be considered a sort of adsorption potential, were obtained 0.4615, 0.4831 and 0.5005 L mg^{-1} for 298 K, 308 K and 318 K respectively. b_T values related to the heat of adsorption, were determined 0.1987, 0.1848, 0.1688 kJ mol^{-1} for 298 K, 308 K and 318 K, respectively. K_T values were indicated that high affinity and b_T values were evidenced of strong interactions between dye molecules and CBA particles which evidence that surface of CBA is heterogeneous. In addition, the correlation coefficient was sufficiently high ($R^2 = 0.99$) to confirm good fitness of the experimental data by this isotherm model (Santhi et al., 2010). The adsorption intensity values (n) calculated with Freundlich model are exceed 1.0 suggest that enhanced adsorption efficiency and development of strong interactions between MB molecules and CBA. Furthermore, the fact that 1/n values are below 1.0 indicate that adsorption of MB on CBA is highly favorable, aligning with previous findings. The K_F constants were found to be 2.4070, 2.5223 and 2.5715 $(mg\ g^{-1})(L\ mg^{-1})^n$ at the 298 K, 308 K and 318 K, respectively. The progressive rise in both K_F and n parameters with increasing temperature were showed that adsorption becomes more efficient at high temperatures, supported that the endothermic nature of the process. The Langmuir model, which assumes monolayer adsorption on a homogeneous surface with a finite number of identical sites (Guo & Briscoe, 2023). The Langmuir constant (K_L), which is reflected the binding site affinity in terms of adsorption process and K_L values were determined to be 0.01365, 0.01986 and 0.02397 L mg^{-1} at 298 K, 308 K and 318 K, respectively. The increased K_L values with the temperature were showed that adsorption is endothermic process. The maximum adsorption capacities (q_{max}) were calculated to be 81.967, 84.746 and 91.743 mg g^{-1} at the 298 K, 308 K and 318 K, respectively. The increase in q_{max} values with increasing temperature were indicated that further confirmation of endothermic process. The Langmuir factor (R_L) is employed to assess the favorability of adsorption. R_L values exceed 1.0, the adsorption process is considered unfavorable, but R_L values between 0 and 1.0 are indicated that favorable adsorption (Yar & Parlayici, 2022). R_L values of MB adsorption on CBA were calculated from 0.747 to 0.957. Since R_L values were varied between the 0–1 values, they were confirmed that process was favorable and suggested that adsorption was irreversible in nature (Kalam et al., 2021). Dubinin–Radushkevich (D–R) isotherm

provided that the estimate of the mean free energy of adsorption (E_{D-R}) per adsorbed MB molecule was employed to analyze the experimental data. The E_{D-R} values were calculated 380.6, 400.3 and 413.4 J mol^{-1} at the 298 K, 308 K and 318 K, respectively. Since determined E_{D-R} values remained below 800 J mol^{-1}, suggested that adsorption was governed by physical interactions. The plots of four isotherm models which were applied to describe MB adsorption onto CBA were shown in Figure 4. The order of applied models the best fitted to data was obtained to Temkin > Freundlich > Dubinin–Radushkevich > Langmuir. Numerous investigations were explored the application of adsorbents derived from various materials for adsorption of MB. Determined removal capacities of MB on different adsorbents were represented in Table 3. The prepared CBA was used in this research because of its low cost and environmental sustainability and it was demonstrated notably higher adsorption capacity for MB in comparison to those reported in previous studies. The obtained results were showed that potential of CBA as an efficient and eco-friendly adsorbent for eliminating pollutants from wastewater. CBA, which is not usually used, is taken in the present study for removal of MB from aqueous solution to investigate the possibility of utilizing it for treatment of wastewater. Therefore, the cost of this removal process is practically due to the cost of transportation of cranberry. Considering the availability of high amount of cranberry as an agricultural waste material, the cost of pollutants removal by this method should be used in treatment of wastewater.

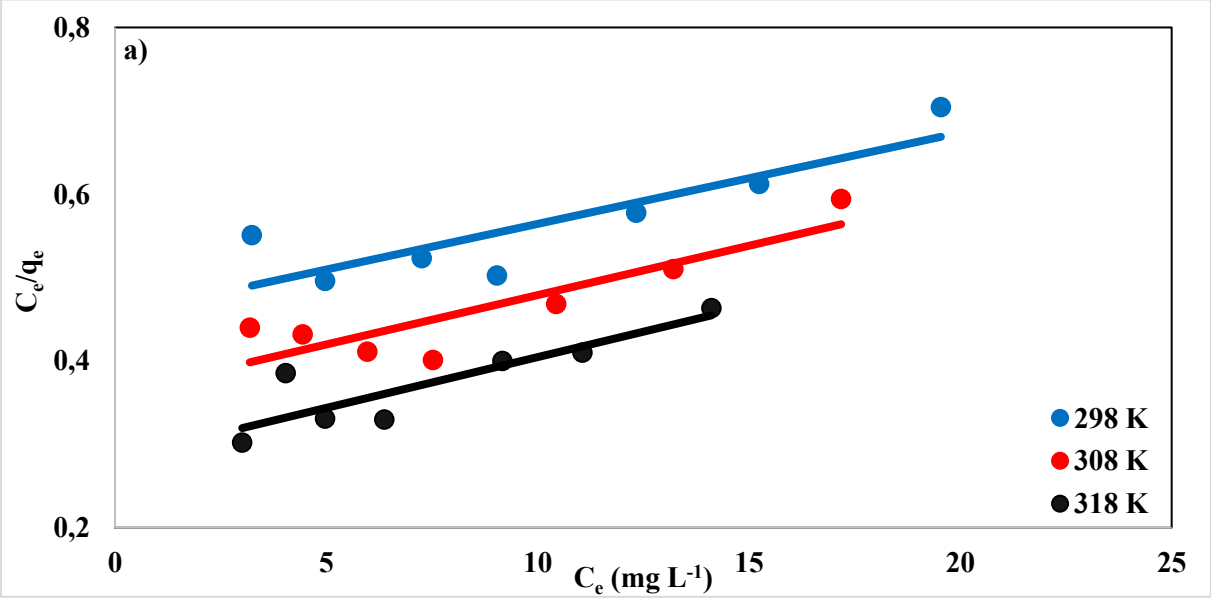

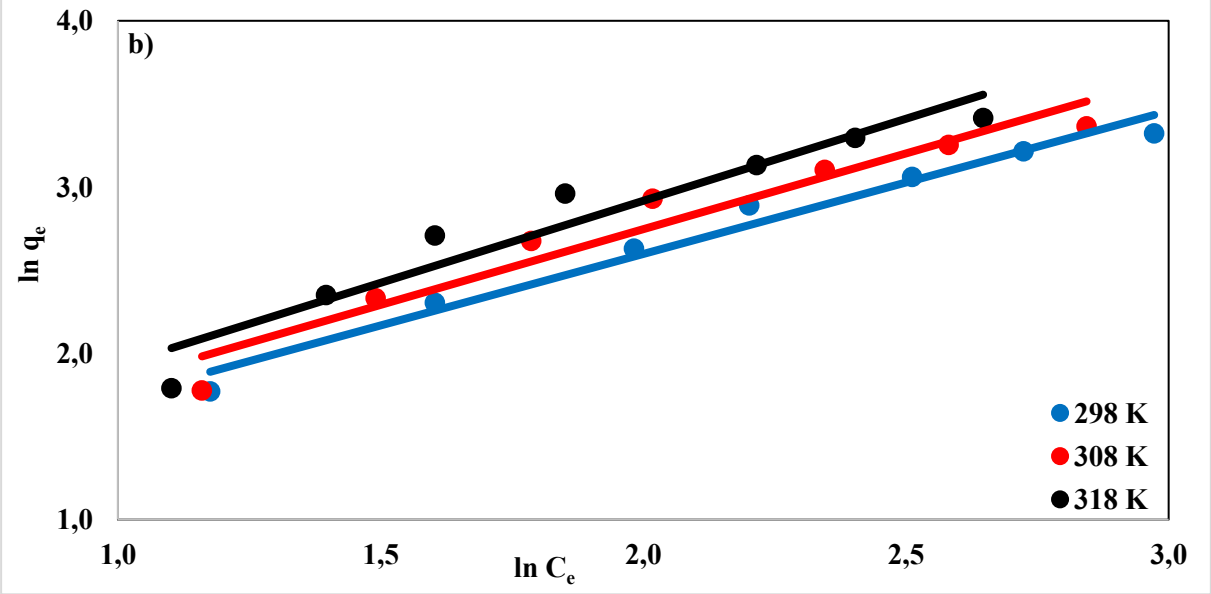

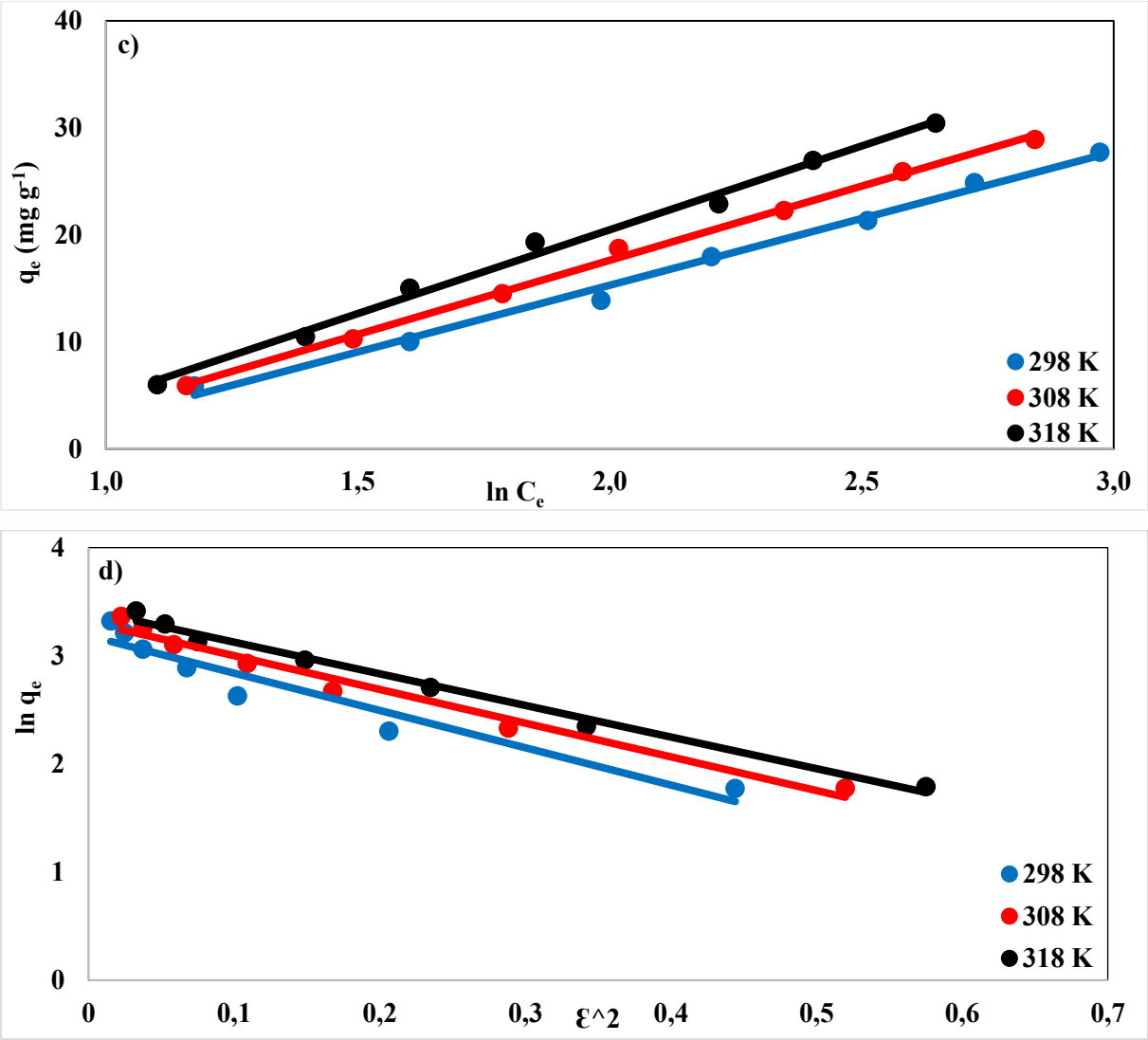

Figure 4. Isotherm plots of MB adsorption on CBA a) Langmuir, b) Freundlich, c) Temkin, d) D-R.

Table 2. Constants of isotherm models for MB adsorption on CBA.

Isotherm / Temperature		**298 K**	**308 K**	**318 K**
Langmuir	K_L (L g^{-1})	0.01365	0.01986	0.02397
	q_m (mg g^{-1})	81.967	84.746	91.743
	R^2	0.7505	0.7794	0.7687
Freundlich	n	1.0134	1.0981	1.1632
	1/n	0.7788	0.7284	0.7162
	K_F (mg g^{-1})(L mg^{-1})	2.4070	2.5223	2.5715
	R^2	0.9753	0.9825	0.9841
Temkin	B_T	12.469	13.857	15.659
	K_T (L g^{-1})	0.4615	0.4831	0.5005
	b_T (kJ mol^{-1})	0.1987	0.1848	0.1688
	R^2	0.9924	0.9974	0.9929
Dubinin-Radushkevich	q_{D-R}	24.1503	27.4481	30.5114
	E_{D-R} (kJ mol^{-1})	0.3806	0.4003	0.4134
	K_{D-R}	3.4522	3.1196	2.9262
	R^2	0.9251	0.9751	0.9685

Table 3. Methylene Blue removal capacities on adsorbents.

Adsorbent type	Adsorption capacity (mg g^{-1})	Reference
Elaeagnus angustifolia seeds	72.00	(Baytar et al., 2021)
Coconut shell	50.60	(Jawad et al., 2020)
Magnetic cellulose/GO composite	70.00	(Shi et al., 2014)
Fe3O4/ZA nanocomposite	40.46	(Mouni et al., 2018)
Treated sawdust	30.11	(Al-Husseiny, 2014)
Coal fly ash	16.53	(Supelano et al., 2020)
Pine wood biochar	25.00	(Lonappan et al., 2016)
Raphia fiber	34.70	(Staron et al., 2019)
Acid modified kaolin	39.92	(Ren et al., 2014)
Ball mill modified biochar	50.27	(Wang et al., 2023)
Tea waste	86.16	(Uddin et al., 2009)
Pearl millet husk	82.37	(Inbaraj et al., 2002)
Cranberry adsorbent (CBA)	91.74	This study

3.4 Kinetic results of MB adsorption on PCA

Adsorption kinetics are studied to understand the underlying mechanisms that govern the process, including chemical interactions, diffusion phenomena and mass transfer effects (Godiya and Ruotolo, 2023). The PFO, PSO and IPD models were applied to obtained data of MB adsorption on CBA. The plots of these kinetic models for 318 K were shown in Figure 5 and obtained parameters of three models for 65 mg L^{-1} initial MB concentration were given in Table 4. The most suitable kinetic model was determined by comparing correlation coefficients (R^2) and PSO model which was exhibited R^2 values close to 1.0, indicated that the highest agreement compared to the PFO and IPD models. The best fit with the PSO model was suggested that involving electron transfer between MB molecules and the CBA surface. The $q_{e,cal}$ values for three kinetic models were showed an increasing trend with rising temperature. These kinetic results were evidenced with previous studies for MB adsorption on different adsorbents (Momina et al., 2020; Ahmed et al., 2019). Figure 5 was showed that kinetic plots used to evaluate the model performance and based on fit to the data, suitability of models were followed order: PSO > PFO > IPD.

Table 4. Parameters of kinetic models of MB adsorption on CBA (MB conc.: 65 mg L^{-1}).

Model / Temperature		298 K	308 K	318 K
$q_{e,exp}$ (mg g^{-1})		24.880	25.895	26.970
PFO kinetic model	k_1 (min^{-1})	0.0348	0.0399	0.0409
	$q_{e,cal}$ (mg g^{-1})	24.511	26.458	27.536
	R^2	0.9065	0.9415	0.9451
PSO kinetic model	k_2 (min^{-1})	0.0124	0.0147	0.0179
	$q_{e,cal}$ (mg g^{-1})	26.667	27.473	28.011
	R^2	0.9982	0.9936	0.9958
IPD Kinetic model	k_{int} (mg $g^{-1}.min^{-0.5}$)	1.5652	1.6415	1.7136
	C (mg g^{-1})	6.576	7.584	10.176
	R^2	0.8721	0.8505	0.8339

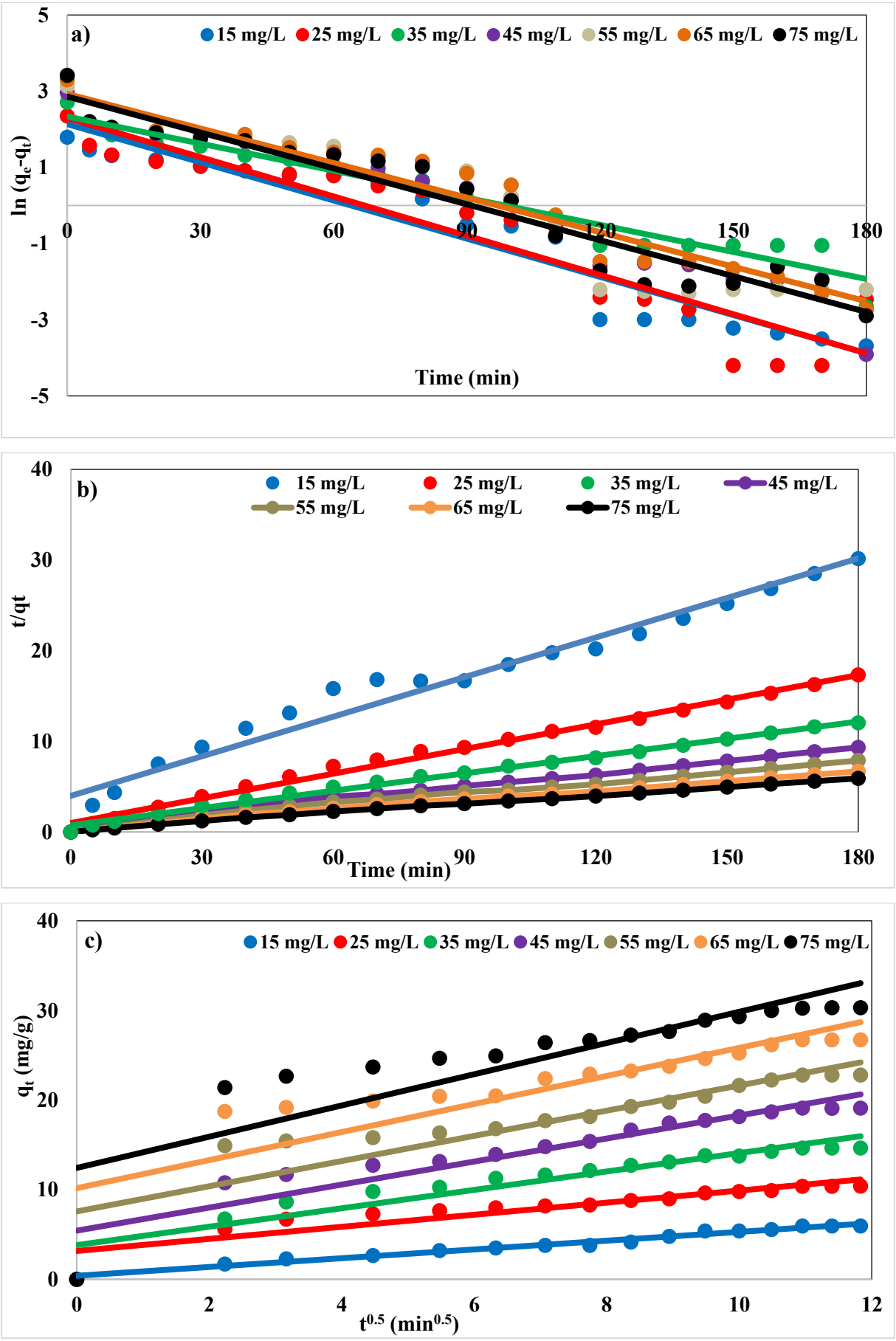

Figure 5. Kinetic model plots for MB adsorption on CBA at the 318 K, a) PFO, b) PSO, c) IPD.

3.5 Thermodynamic results for MB adsorption on CBA

Gibbs free energy (ΔG°), enthalpy (ΔH°) and entropy (ΔS°) values were evaluated to behaviour of MB adsorption on CBA. These values, which were obtained with Eq. (15) – (17) and the results were given in Table 5. The ΔG° values were found to be –1711.96, –2327.06 and –2942.16 J mol^{-1}, for 65 mg L^{-1} initial MB concentration, at 298 K, 308 K and 318 K respectively. The ΔG◦ values which were obtained at three temperatures were indicated that adsorption is both feasible and spontaneous (Table 5). The increasing ΔG° values with rising temperature were suggested that enhanced adsorption efficiency at high temperatures. The ΔH° and ΔS° values were determined to be 16.618 kJ mol^{-1} and 61.51 J $mol^{-1}\cdot K^{-1}$, respectively, confirmed that the endothermic nature of process. The positive enthalpy values were implied that adsorption is primarily driven by physical forces and positive entropy values were reflected that an increase in randomness at the solid–liquid interface, indicated that strong affinity between CBA and MB molecules (Cordova Estrada et al., 2021). The activation energy (E_A) explain the selection of physical or chemical adsorption. A linear plot of lnKd versus 1/T with slope $-E_A/R$ for the adsorption of MB on CBA was drawn to determine the E_A value from slope which were given in Figure 6 for seven initial MB concentrations. E_A for this removal process was derived from Arrhenius equation which was calculated as 14.44 kJ mol^{-1}. Since obtained E_A value was below 40 kJ mol^{-1}, supported that MB adsorption on CBA was governed by the physical adsorption mechanism.

Table 5. Thermodynamic parameters of MB adsorption on CBA.

MB conc. (mg L^{-1})	ΔG° (J mol^{-1})			ΔH°	ΔS°	
	298 K	308 K	318 K	(J mol^{-1})	(J $mol^{-1}.K^{-1}$)	R^2
15	-1453.20	-1624.10	-1795.00	3639.62	17.09	0.9895
25	-1742.55	-2135.15	-2527.75	9956.93	39.26	0.9985
35	-1376.03	-1908.62	-2441.22	14495.46	53.26	0.9999
45	-1195.04	-1764.84	-2334.64	15785.79	56.98	0.9995
55	-830.04	-1410.44	-1990.84	16465.88	58.04	0.9961
65	-1711.96	-2327.06	-2942.16	16618.02	61.51	0.9952
75	-1607.84	-2267.74	-2927.64	18057.18	65.99	0.9842

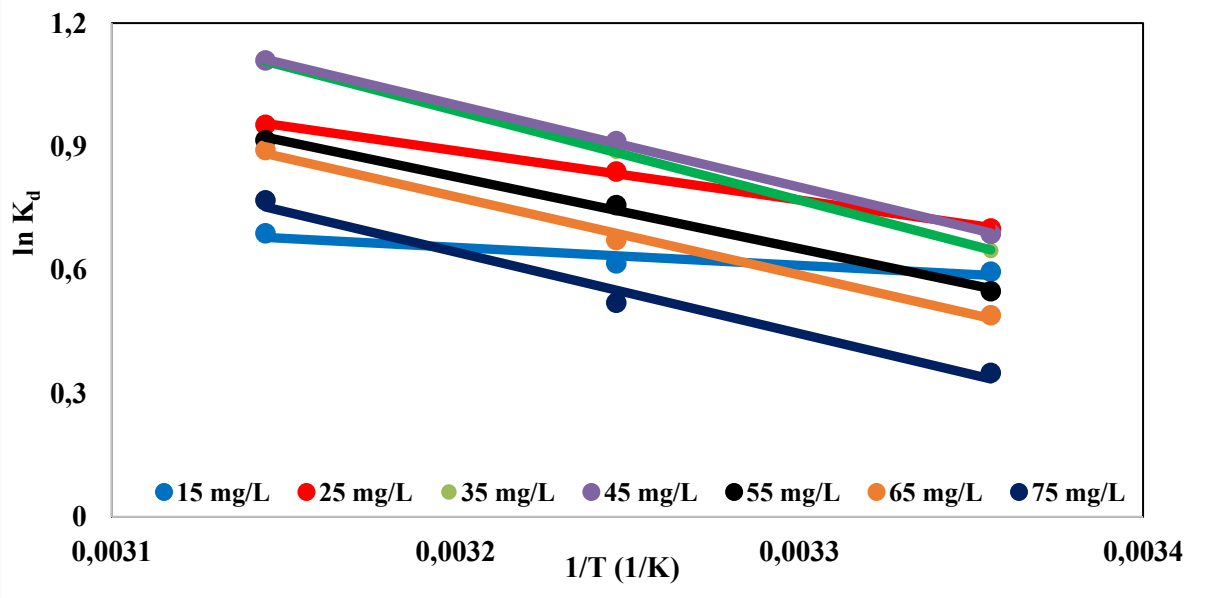

Figure 6. Van't Hoff plots for MB adsorption on CBA.

4. Conclusion

In this study, cranberry based adsorbent (CBA) was used for the removal of Methylene Blue (MB) from aqueous solutions. Batch adsorption experiments were carried out with seven initial MB concentrations and three different temperatures to evaluate the performance of CBA. The adsorption capacities of CBA for MB with the concentration ranges of 15–75 mg L^{-1} were found to be 5.88–27.73 mg g^{-1} at 298 K, 5.95–28.91 mg g^{-1} at 308 K and 6.01–30.45 mg g^{-1} at 318 K. Isotherm modeling studies were performed with four models and Temkin isotherm was provided the best fit to experimental data compared to other applied isotherm models. The correlation coefficients (R^2) of the Temkin model were consistently of the highest and isotherm constants were showed an increase trend with temperature, indicated that enhanced adsorption affinity at elevated thermal conditions. The maximum adsorption capacities (q_m) of CBA were calculated as 81.967 mg g^{-1} at 298 K, 84.746 mg g^{-1} at 308 K and 91.743 mg g^{-1} at 318 K, further confirming the endothermic nature of the adsorption process. Kinetic modeling was performed using PFO, PSO and IPD models and the results were demonstrated that adsorption process adhered most closely to the PSO kinetic model, with the highest correlation coefficients (R^2). Determined all kinetic parameters were exhibited an increase trend with increase temperature, supported that the temperature dependence of the adsorption mechanism. Thermodynamic parameters of MB adsorption on CBA were also determined. The negative values of Gibbs free energy changes ($\Delta G°$) calculated for three temperatures were indicated that feasibility and spontaneity of process. The positive enthalpy changes were showed that endothermic process and positive entropy changes were established that randomness at CBA–MB interface with high affinity of CBA to MB. Overall, the results of this research suggested that CBA is a promising and sustainable low-cost adsorbent for effective removal of dyes from wastewater.

Authors' Contributions

Ali Rıza Kul: Experimental, Methodology, Formal analysis, Resources, Writing—original draft, Writing—review & editing.
Adnan Aldemir: Conceptualization, Methodology, Supervision, Software, Writing—original draft, Writing—review & editing, Formal analysis, Visualization, Validation, Resources.

Declaration of Competing Interests

The authors declare that they have no known competing financial interests or personal relationships that could have appeared to influence the work reported in this paper.

Statement on Research and Publication Ethics

The authors of this article declare that they have complied with research and publication ethics (YÖK Scientific Research and Ethics Regulation (yok.gov.tr), Declaration of Helsinki, Committee on Publication Ethics (COPE), WAME).

Ethics Committee Statement

The author(s) of this article declare that the materials and methods used in their study did not require ethics committee approval and/or any legal or special permission.

Use of Artificial Intelligence

The author(s) declare that they did not use any type of generative artificial intelligence in the writing of this article or in the creation of images, graphics, tables, or their corresponding captions.

References

Ahmad, M. A., Ahmad, N., & Bello, O. S. (2015). Modified durian seed as adsorbent for the removal of methyl red dye from aqueous solutions. *Applied Water Science, 5,* 407–423. https://doi.org/10.1007/s13201-014-0208-4

Ahmed, M. J., Okoye, P. U., Hummadi, E. H., & Hameed, B. H. (2019). High-performance porous biochar from the pyrolysis of natural and renewable seaweed (Gelidiella acerosa) and its application for the adsorption of methylene blue. *Bioresource Technology, 278,* 159-164. https://doi.org/10.1016/j.biortech.2019.01.054

Aigbe, U. O., Ukhurebor, K. E., Onyancha, R. B., Osibote, O. A., Darmokoesoemo, H., & Kusuma, H. S. (2021). Fly ash-based adsorbent for adsorption of heavy metals and dyes from aqueous solution: a review. *Journal of Material Research Technology, 14,* 2751–2774. https://doi.org/10.1016/j.jmrt.2021.07.140

Aldemir, A., Hakkıtanır, E., & Özgüven, A. (2021). Determination of optimum treatment conditions for paint industry wastewater with the coagulation/flocculation method. *Desalination & Water Treatment, 211,* 165–176. https://doi.org/10.5004/dwt.2021.26624

Aldemir, A., Turan, A., Kul, A.R., & Koyuncu, H., (2023). Comprehensive investigation of Basic Red 46 removal by pinecone adsorbent: experimental, isotherm, kinetic and thermodynamic studies. *International Journal of Environmental Science & Technology, 383(1)*, 1-26. https://doi.org/10.1007/s13762-022-04456-6

Al-Husseiny, & H. A. (2014). Adsorption of methylene blue dye using low cost adsorbent of sawdust: batch and continues studies. *Journal of University of Babylon, 22(2),* 296-310.

Alsaffar, M. A., Rahman, M. A., Mageed, A. K., Ali, S. A. K., Lutfee, T., Adnan, S. W., & Shakir, H. A. A. (2023). Electrochemical removal of dye from a tanning process industrial wastewater. *Chemical Papers, 77,* 6311–6318. https://doi.org/10.1007/s11696-023-02940-y

Alver, E., Metin, A. Ü., & F. Brouers, F. (2020). Methylene blue adsorption on magnetic alginate/rice husk bio-composite. *International Journal of Biological Macromolecules, 154,* 104-113. https://doi.org/10.1016/j.ijbiomac.2020.02.330

Ayhan, N. N., Aldemir, A., & Özgüven, A. (2024). Treatment of petroleum refinery wastewater by chemical coagulation method: determination of optimum removal conditions using experimental design. *Brazilian Journal of Chemical Engineering, 41,* 121-137. https://doi.org/10.1007/s43153-023-00358-3

Baytar, O., Ceyhan, A. A., & Şahin, O. (2021). Production of activated carbon from Elaeagnus angustifolia seeds using H3PO4 activator and methylene blue and malachite green adsorption. *International Journal of Phytoremediation, 23 (7),* 693–703. https://doi.org/10.1080/15226514.2020.1849015

Bhatti, H. N., Safa, Y., Yakout, S. M., Shair, O. H., Iqbal, M., & Nazir, A. (2020). Efficient removal of dyes using carboxymethyl cellulose/alginate/polyvinyl alcohol/rice husk composite: Adsorption/desorption, kinetics and recycling studies. *International Journal of Biological Macromolecules, 150,* 861-870. https://doi.org/10.1016/j.ijbiomac.2020.02.093

Chowdhury, M. F., Kim, C. M., & Jang, A. (2023). High-efficient and rapid removal of anionic and cationic dyes using a facile synthesized sole adsorbent NiAlFe-layered triple hydroxide (LTH). *Chemosphere, 332,* 138878. https://doi.org/10.1016/j.chemosphere.2023.138878

Cordova Estrada, A. K., Lozano, F. Cordova, Lara Díaz, R. A. (2021). Thermodynamics and kinetic studies for the adsorption process of methyl orange by magnetic activated carbons. *Air Soil Water Research, 14.* https://doi.org/10.1177/11786221211013336/

Daneshvar, E., Vazirzadeh, A., Niazi, A., Kousha, M., Naushad, M., & Bhatnagar, A. (2017). Desorption of methylene blue dye from brown macroalga: effects of operating parameters, isotherm study and kinetic modeling. *Journal of Cleaner Production, 152,* 443–453. https://doi.org/10.1016/j.jclepro.2017.03.119.

Das, T. K., Ghosh, S. K., & Das, N. C. (2023). Green synthesis of a reduced graphene oxide/silver nanoparticles-based catalyst for degradation of a wide range of organic pollutants. *Nano-Structures & Nano-Objects, 34,* 100960. http://dx.doi.org/10.2139/ssrn.4224529

Demirci, G. V., Baig, M. T., & Kayan, A. (2024). UiO-66 MOF/Zr-di-terephthalate/cellulose hybrid composite synthesized via sol-gel approach for the efficient removal of methylene blue dye.

International Journal of Biological Macromolecules, 283, 1–16. https://doi.org/10.1016/j.ijbiomac.2024.137950

Dhaouadi, F., Sellaoui, L., Dotto, G. L., Bonilla-Petriciolet, A., Erto, A., & Lamine, A. B. (2020). Adsorption of methylene blue on comminuted raw avocado seeds: Interpretation of the effect of salts via physical monolayer model. *Journal of Molecular Liquids, 305,* 1-8. https://doi.org/10.1016/j.molliq.2020.112815

Dutta, S. B. Gupta, B., Srivastava, S. K., & Gupta, A. K. (2021). Recent advances on the removal of dyes from wastewater using various adsorbents: A critical review. *Materials Advances, 2(14)*, 4497–4531. https://doi.org/10.1039/d1ma00354b

Godiya, C. B., & Ruotolo, L. A. M. (2023). Plant leaves waste for removal of metal ions. *Emerging Techniques for Treatment Toxic Metals from Wastewater,* 47–82. https://doi.org/10.1016/B978-0-12-822880-7.00014-5.

Guo, X., & Briscoe, W. H. (2023). Molecular interactions, elastic properties and nanostructure of Langmuir bacterial-lipid monolayers: towards solving the mystery in bacterial membrane asymmetry. *Current Opinion Colloid Interface Science, 67*, 101731. https://doi.org/10.1016/j.cocis.2023.101731.

Ho, Y. S., & Mckay, G. (1998). Kinetic models for the sorption of dye from aqueous solution by wood. *Process Safety and Environmental Protection, 76*, 183-191.

Inbaraj, B. S., Selvarani, K., & Sulochana, N. (2002). Evaluation of a carbonaceous sorbent prepared from pearl millet husk for its removal of basic dyes. *Journal of Scientific Industrial Research, 61*, 971–978.

Jawad, A. H., Razuan, R., Appaturi, J. N., & Wilson, L. D. (2019). Adsorption and mechanism study for methylene blue dye removal with carbonized watermelon (Citrullus lanatus) rind prepared via one-step liquid phase H2SO4 activation. *Surfaces and Interfaces, 16*, 76-84. https://doi.org/10.1016/j.surfin.2019.04.012

Jawad, A. H., Abdulhameed, A. S., & Mastuli, M. S. (2020). Acid-factionalized biomass material for methylene blue dye removal: a comprehensive adsorption and mechanism study. *Journal of Taibah University Science, 14(1),* 305–313. https://doi.org/10.1080/16583655.2020.1736767

Joseph, J., Radhakrishnan, R. C., Johnson, J. K., Joy, S. P., & Thomas, J., (2020). Ion-exchange mediated removal of cationic dye-stuffs from water using ammonium phosphomolybdate. *Materials Chemistry and Physics, 242*, 1-8. https://doi.org/10.1016/j.matchemphys.2019.122488

Kalam, S., Abu-Khamsin, S. A., Kamal, M. S., & Patil, S. (2021). Surfactant adsorption isotherms: a review. *ACS Omega, 6(48)*, 32342–32348. https://doi.org/10.1021/ACSOMEGA.1C04661/ASSET/IMAGES/MEDIUM/AO1C04661_M047.GIF

Kang, Y.-G., Yoon, H., Lee, C.-S., Kim, E.-J., & Chang, Y.-S. (2019). Advanced oxidation and adsorptive bubble separation of dyes using MnO2-coated Fe3O4 nanocomposite. *Water Research, 151*, 413-422. https://doi.org/10.1016/j.watres.2018.12.038

Katheresan, V., Kansedo, J., & Lau, S. Y. (2018). Efficiency of various recent wastewater dye removal methods: A review. *Journal of Environmental Chemical Engineering, 6(1)*, 4676–4697. https://doi.org/10.1016/j.jece.2018.06.060

Khan, I., Saeed, K., Zekker, I., Zhang, B., Hendi, A. H., Ahmad, A., Ahmad, S., Zada, N., Ahmad, H., Shah, L. A., Shah, T., & Khan, I. (2022). Review on methylene blue: its properties, uses, toxicity and photodegradation. *Water, 14*, 242–271. https://doi.org/10.3390/w14020242

Kul, A. R., Koyuncu, H., Turan, A., & Aldemir, A. (2023). Comparative research of isotherm, kinetic and thermodynamic studies for neutral red adsorption by activated carbon prepared from apple peel. *Water Air Soil Pollution, 383,* 1-26. https://doi.org/10.1007/s11270-023-06392-8

Kul, A. R., & Aldemir, A. (2025). An investigation of aniline removal performance by the activated carbon prepared from biomass conversion: adsorption results of isotherm, kinetic and thermodynamic studies. *Biomass Conversion & Biorefinery, 15*, 19915-19930. https://doi.org/10.1007/s13399-024-06433-0

Lagergren, S., & Svenska, B. K. (1898). Zur theorie der sogenannten adsorption geloester stoffe, *Veternskapsakad Handlingar, 24*, 1-39.

Liu, Y., Liu, Y., Qu, R., Ji, C., & Sun, C., (2020). Comparison of adsorption properties for anionic dye by metal organic frameworks with different metal ions. *Colloids and Surfaces A: Physicochemical and Engineering Aspects, 586*, 1-7. https://doi.org/10.1016/j.colsurfa.2019.124259

Lonappan, L., Rouissi, T., Das, R. K., Brar, S. K., Ramirez, A. A., Verma, M., Surampalli, R. Y., & Valero, J. R. (2016). Adsorption of methylene blue on biochar microparticles derived from different waste materials. *Waste Management, 49*, 537–544. https://doi.org/10.1016/j.wasman.2016.01.015

Misran, E., Supardan, M. D., Iryani, D. A., Pramananda, V., Sihombing, A. F., & Sitorus, D. V. (2024). Ultrasonic assisted adsorption of methylene blue using blood clam shell as a low-cost adsorbent. *Results in Engineering, 23,* 1–13. https://doi.org/10.1016/j.rineng.2024.102715

Mladenov, N., Dodger, N. G., Steinberg, L., Richardot, W., Johnson, J., Martincigh, B. S., Buckley, C., Lawrence, T., & Hoh, E. (2022). Persistence and removal of trace organic compounds in centralized and decentralized wastewater treatment systems. *Chemosphere 286*, 131621. https://doi.org/10.1016/j.chemosphere.2021.131621

Momina, Mohammad, S., & Suzylawati, I. (2020). Study of the adsorption/desorption of MB dye solution using bentonite adsorbent coating. *Journal of Water Process Engineering, 34*, 101155 https://doi.org/10.1016/j.jwpe.2020.101155

Mouni, L., Belkhiri, L., Bollinger, J.-C., Bouzaza, A., Assadi, A., Tirri, A., Dahmoune, F., Madani, K., & Remini, H. (2018). Removal of Methylene Blue from aqueous solutions by adsorption on Kaolin: kinetic and equilibrium studies. *Applied Clay Science, 153*, 38–45. https://doi.org/10.1016/j.clay.2017.11.034

Muniyasamy, A., Sivaporul, G., Gopinath, A., Lakshmanan, R., Altaee, A., Achary, A., & Chellam, P. V. (2020). Process development for the degradation of textile azo dyes (mono-, di-, poly-) by advanced oxidation process - ozonation: experimental & partial derivative modelling approach. *Journal of Environmental Management, 265*, 1-10. https://doi.org/10.1016/j.jenvman.2020.110397

Oladoye, P. O., Ajiboye, T. O., Omotola, E. O., & Oyewola, O. J. (2022). Methylene blue dye: toxicity and potential elimination technology from wastewater. *Results in Engineering, 16*, 1–17. https://doi.org/10.1016/j.rineng.2022.100678

Parlayici, S., & Aras, A. (2024). Synthesis of a novel green biopolymer-based composites beads for removal of methylene blue from aquatic medium: isotherm, thermodynamic and kinetic investigation. *Polymer Bulletin, 81(7)*, 6603–6640. https://doi.org/10.1007/s00289-024-05164-6

Peighambardoust, S. J., Boffito, D. C., Foroutan, R., & Ramavandi, B. (2022). Sonophotocatalytic activity of sea sediment@400/ZnO catalyst to remove cationic dyes from wastewater. *Journal of Molecular Liquids, 367*, 120478 https://doi.org/10.1016/j.molliq.2022.120478

Pereira, L. A., Couto, A. B., Almeida, D. A. L., & Ferreira, N. G. (2020). Singular properties of boron-doped diamond/carbon fiber composite as anode in Brilliant Green dye electrochemical degradation. *Diamond and Related Materials, 103*, 1-7. https://doi.org/10.1016/j.diamond.2020.107708

Ren, X. L., Shu, X. Q., Geng, W. G., Li, P., & Xu, Y. E. (2024). A study on the adsorption of methylene blue by acid-modified coal measures kaolin. *Processes, 12*, 773. https://doi.org/10.3390/pr12040773

Salleh, M. A. M., Mahmoud, D. K., Karim, W. A. W. A., & Idris, A. (2011). Cationic and anionic dye adsorption by agricultural solid wastes: a comprehensive review. *Desalination, 280(1-3)*, 1–13. https://doi.org/10.1016/j.desal.2011.07.019

Santhi, T., Manonmani, S., & Smitha, T. (2010). Kinetics and isotherm studies on cationic dyes adsorption onto Annona Squmosa seed activated carbon. *International Journal of Engineering Science & Technology, 2*, 287–295.

Shi, H., Li, W., Zhong, L., & Xu, C. (2014). Methylene blue adsorption from aqueous solution by magnetic cellulose/graphene oxide composite: equilibrium, kinetics and thermodynamics. *Industrial Engineering Chemistry Research, 53*, 1108–1118. https://doi.org/10.1021/ie4027154

Singh, R. L., Singh, P. K., & Singh, R. P. (2015). Enzymatic decolorization and degradation of azo dyes – a review. *International Biodeterioration & Biodegradation*, 104, 21–31. https://doi.org/10.1016/j.ibiod.2015.04.027

Spagnoli, A. A., Giannakoudakis, D. A., & Bashkova, S. (2017). Adsorption of methylene blue on cashew nut shell based carbons activated with zinc chloride: the role of surface and structural parameters. *Journal of Molecular Liquids, 229*, 465–471. https://doi.org/10.1016/j.molliq.2016.12.106

Staron, P., Chwastowski, J., & Banach, M. (2019). Sorption behaviour of methylene blue from aqueous solution by raphia fibers. *International Journal of Environmental Science & Technology, 16*, 8449–8460. https://doi.org/10.1007/s13762-019-02446-9

Supelano, G. I., G´omez Cuaspud, J. A., Moreno-Aldana, L. C., Ortiz, C., Trujillo, C. A., Palacio, C. A., Parra Vargas, C. A., & Mejía G´omez, J. A. (2020). Synthesis of magnetic zeolites from recycled fly ash for adsorption of methylene blue. *Fuel, 263*, 116800. https://doi.org/10.1016/j.fuel.2019.116800

Uddin, M. T., Islam, M. A., Mahmud, S., & Rukanuzzaman, M. (2009). Adsorptive removal of methylene blue by tea waste. *Journal of Hazardous Materials, 164*, 53–60. https://doi.org/10.1016/j.jhazmat.2008.07.131

Wang, J., & Guo, X. (2020). Adsorption isotherm models: classification, physical meaning, application and solving method. *Chemosphere, 258*, 127279. https://doi.org/10.1016/j.chemosphere.2020.127279

Wang, J. X., Tan, Y. F., Yang, H. J., Zhan, L. L., Sun, G. W., & Luo, L. (2023). On the adsorption characteristics and mechanism of methylene blue by ball mill modified biochar. *Scientific Reports, 13*, 21174. https://doi.org/10.1038/s41598-023-48373-1

Weber, W. J., & Morris, J. C. (1963). Kinetics of adsorption on carbon from solution. *Journal of the Sanitary Engineering Division, 89*, 31-60.

Yagub, M. T., Sen, T. K., Afroze, S., & Ang, H. M. (2014). Dye and its removal from aqueous solution by adsorption: a review. *Advances Colloid and Interface Science, 209*, 172–184. https://doi.org/10.1016/j.cis.2014.04.002

Yar, A., & Parlayici, S. (2022). Carbon nanotubes/polyacrylonitrile composite nanofiber mats for highly efficient dye adsorption. *Colloids Surf. A Physicochemical Engineering Asp. 651*, 129703. https://doi.org/10.1016/j.colsurfa.2022.129703

Zeghioud, H., Fryda, L., Mahieu, A., Visser, R., & Kane, A. (2022). Potential of flax shives and beech wood-derived biochar in methylene blue and carbamazepine removal from aqueous solutions. *Materials, 15*, 2824. https://doi.org/10.3390/ma15082824

Zhang, P., Liu, B., Zhao, T., Yu, J., Ye, X., & Chen, X. (2024). Degradation of typical nitrogen-heterocyclic compounds in coal gasification wastewater via catalytic ozonation processes. *Water Air Soil Pollution, 235(793)*, 1–11. https://doi.org/10.1007/s11270-024-07516-4